

Photophysics of Tungsten and Molybdenum Arylcarbyne Complexes. Observation of the Lowest Excited State by Laser Flash Photolysis

Thomas K. Schoch, Andrea D. Main, Richard D. Burton, Lucian A. Lucia,
Edward A. Robinson, Kirk S. Schanze,* and Lisa McElwee-White*

Department of Chemistry, University of Florida, P.O. Box 117200, Gainesville, Florida 32611

Received August 9, 1995[⊗]

The photophysics of the series of tungsten and molybdenum arylcarbyne complexes $\text{Cp}(\text{CO})\{\text{P}(\text{OMe})_3\}\text{M}\equiv\text{C}-\text{Ar}$ (**1a**, M = W, Ar = phenyl; **1b**, M = Mo, Ar = phenyl; **1c**, M = W, Ar = *o*-tolyl; **1d**, M = W, Ar = 2-naphthyl) has been examined by using absorption, emission, and transient absorption spectroscopy. Extended Hückel calculations indicate that the lowest excited state of these arylcarbyne complexes is based on a $d(\text{M}) \rightarrow \pi^*(\text{M}\equiv\text{C}-\text{Ar})$ configuration. Consistent with this prediction, each of the complexes displays a weak, mid-visible absorption band which is attributed to the $d \rightarrow \pi^*$ transition. The tungsten complexes **1a**, **1c**, and **1d** also exhibit red luminescence with a lifetime in the 100–200 ns regime. Nanosecond laser flash photolysis studies indicate that the arylcarbyne complexes display a strong transient absorption with a maximum in the 400–450 nm region. Close correspondence between decay lifetimes obtained by luminescence and transient absorption indicate that the transient absorption may be assigned to the $d \rightarrow \pi^*$ excited state.

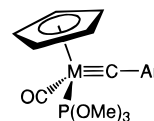
Introduction

The photochemistry of low-valent metal carbyne complexes has been of interest due to their unique photophysical properties and excited state reactivity.^{1–3} Although photolysis of organometallic compounds typically results in ligand loss as the primary photoprocess due to population of a metal–ligand antibonding orbital via excitation of the $d-d$ manifold,⁴ examples of metal carbyne photochemistry include transformations which convert the carbyne moiety to other organic ligands.⁵

Photochemical electron transfer has been shown to activate $18 e^-$ complexes toward reactivity,⁶ and this strategy has proven effective for metal carbynes. In previous work, a photooxidation reaction involving irreversible electron transfer from a series of tungsten and molybdenum aryl- and alkylcarbynes to halogenated solvents was observed.² Following generation of the carbyne radical cation, both metal-centered reactions typical of metal radicals and unusual ligand-centered processes ensue.⁷

The present report describes continuation of the photophysical studies of metal carbyne complexes of the type $\text{Cp}(\text{CO})-$

$\{\text{P}(\text{OMe})_3\}\text{M}\equiv\text{C}-\text{R}$, where M = Mo or W and R = aryl (complexes **1a–d**).² These complexes display weak absorption



1a: M = W, Ar = phenyl **1c**: M = W, Ar = *o*-tolyl
1b: M = Mo, Ar = phenyl **1d**: M = W, Ar = 2-naphthyl

bands in the visible region and long-lived luminescence. The low-energy absorption and luminescence of the carbyne complexes involve an excited state manifold which derives from a $d(\text{M}) \rightarrow \pi^*(\text{M}\equiv\text{C}-\text{R})$ excitation that was originally described in the literature as MLCT¹ although its characteristics are consistent with considerable $d-d$ character (*vide infra*).^{1–3} Nanosecond laser flash photolysis studies of the $\text{M}\equiv\text{C}-\text{R}$ complexes reveal that this excited state displays a strong mid-visible absorption, which provides a unique means to study the excited state dynamics and electronic structure of the carbyne complexes.

Results

Synthesis and Characterization of $\text{Cp}(\text{CO})\{\text{P}(\text{OMe})_3\}\text{M}\equiv\text{C}-\text{R}$ Complexes. The carbyne complexes $\text{Cp}(\text{CO})-$

* Authors to whom correspondence should be sent. E-mail: lmwhite@chem.ufl.edu or kschanze@chem.ufl.edu.

[⊗] Abstract published in *Advance ACS Abstracts*, November 1, 1996.

- (1) (a) Bocarsly, A. B.; Cameron, R. E.; Rubin, H. D.; McDermott, G. A.; Wolff, C. R.; Mayr, A. *Inorg. Chem.* **1985**, *24*, 3976–3978. (b) Bocarsly, A. B.; Cameron, R. E.; Mayr, A.; McDermott, G. A. In *Photochemistry and Photophysics of Coordination Compounds*; Yersin, H., Volger, A., Eds.; Springer-Verlag: Berlin, 1987; p 213.
- (2) Carter, J. D.; Kingsbury, K. B.; Wilde, A.; Schoch, T. K.; Leep, C. J.; Pham, E. K.; McElwee-White, L. *J. Am. Chem. Soc.* **1991**, *113*, 2947–2954.
- (3) Trammell, S.; Sullivan, B. P.; Hodges, L. M.; Harmon, W. D.; Smith, S. R.; Thorp, H. H. *Inorg. Chem.* **1995**, *34*, 2791–2792.
- (4) Geoffroy, G. L.; Wrighton, M. S. *Organometallic Photochemistry*; Academic Press: New York, 1976.
- (5) (a) Beevor, R. G.; Freeman, M. J.; Green, M.; Morton, C. E.; Orpen, A. G. *J. Chem. Soc., Dalton Trans.* **1991**, 3021–3030. (b) Sheridan, J. B.; Pourreau, D. B.; Geoffroy, G. L.; Rheingold, A. L. *Organometallics* **1988**, *7*, 289–294. (c) Mayr, A.; Asaro, M. F.; Glines, T. J. *J. Am. Chem. Soc.* **1987**, *109*, 2215–2216. (d) Green, M. *J. Organomet. Chem.* **1986**, *300*, 93–109.
- (6) Giannotti, C.; Gaspard, S.; Krausz, P. In *Photoinduced Electron Transfer, Part D. Photoinduced Electron Transfer Reactions: Inorganic Substrates and Applications*; Fox, M. A., Chanon, M., Eds.; Elsevier: Amsterdam, 1988; pp 200–240.
- (7) (a) Schoch, T. K.; Orth, S. D.; Zerner, M. C.; Jørgensen, K. A.; McElwee-White, L. *J. Am. Chem. Soc.* **1995**, *117*, 6475–6482. (b) McElwee-White, L.; Kingsbury, K. B.; Carter, J. D. *J. Photochem. Photobiol. A: Chem.* **1994**, *80*, 265–270. (c) Mortimer, M. D.; Carter, J. D.; McElwee-White, L. *Organometallics* **1993**, *12*, 4493–4498. (d) Kingsbury, K. B.; Carter, J. D.; Wilde, A.; Park, H.; Takusagawa, F.; McElwee-White, L. *J. Am. Chem. Soc.* **1993**, *115*, 10056–10065. (e) McElwee-White, L.; Kingsbury, K. B.; Carter, J. D. In *Photosensitive Metal-Organic Systems. Mechanistic Principles and Applications*; Kutal, C., Serpone, N., Eds.; Advances in Chemistry 238; American Chemical Society: Washington, DC, 1993; pp 335–349. (f) Carter, J. D.; Schoch, T. K.; McElwee-White, L. *Organometallics* **1992**, *11*, 3571–3578.
- (8) (a) Fischer, E. O.; Maasböl, A. *Chem. Ber.* **1967**, *100*, 2445–2456. (b) Mayr, A.; Dorries, A. M.; McDermott, G. A.; Van Engen, D. *Organometallics* **1986**, *5*, 1504–1506. (c) McDermott, G. A.; Dorries, A. M.; Mayr, A. *Organometallics* **1987**, *6*, 925–931.

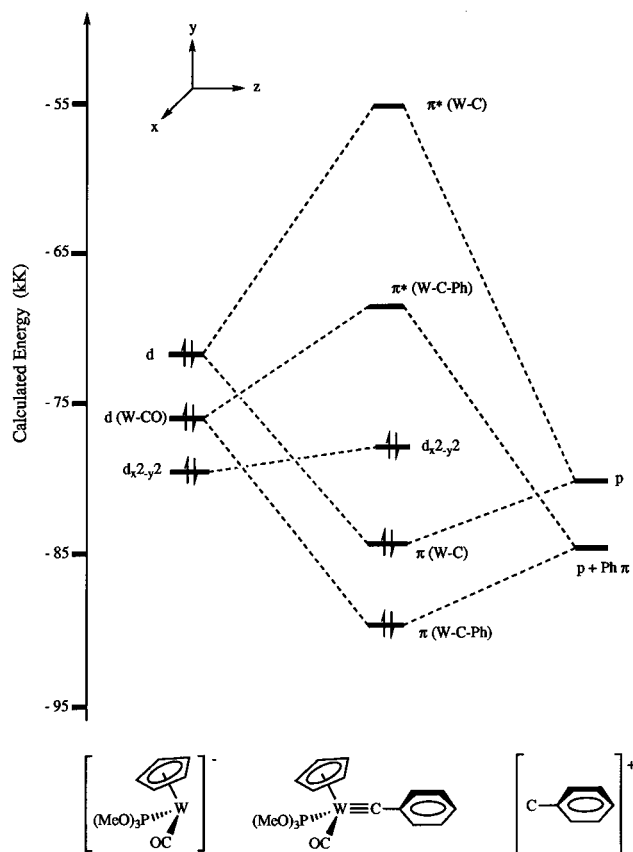


Figure 1. Orbital mixing diagram for $\text{Cp}(\text{CO})\{\text{P}(\text{OMe})_3\}\text{W}\equiv\text{C}-\text{Ph}$ (**1a**). Orbital energies are derived from extended Hückel calculations.

$\{\text{P}(\text{OMe})_3\}_3\text{M}\equiv\text{C}-\text{Ph}$ ($\text{W} = \mathbf{1a}$, $\text{Mo} = \mathbf{1b}$) and $\text{Cp}(\text{CO})\{\text{P}(\text{OMe})_3\}\text{W}\equiv\text{C}(o\text{-Tol})$ (**1c**) were prepared as described previously.^{2,8} Preparation of the naphthylcarbyne complex $\text{Cp}(\text{CO})\{\text{P}(\text{OMe})_3\}\text{W}\equiv\text{C}(2\text{-Np})$ (**1d**) involved an analogous route. The tris(phosphite) complex $\text{Cl}(\text{CO})\{\text{P}(\text{OMe})_3\}_3\text{W}\equiv\text{C}(2\text{-Np})$ (**2d**) was prepared by the reaction of $[(\text{CO})_5\text{W}(\text{CO}\{2\text{-Np}\})]\text{[NMe}_4]$ (**3d**) with oxalyl chloride, followed by addition of excess trimethyl phosphite to give the impure tris(phosphite) complex **2d**. Reaction of **2d** with fresh sodium cyclopentadienide (CpNa) led to displacement of the chloride anion and two $\text{P}(\text{OMe})_3$ ligands to yield **1d**. The crude **1d** required more extensive purification than is necessary for **1a-c**, but was ultimately isolated in 20% yield. Spectroscopic data for **1d** are given in the Experimental Section.

Electronic Structure of 1a and 1b. As an aid to interpreting the spectra of **1a-d**, extended Hückel calculations⁹ were performed on **1a** and **1b**. Although the results of these one-electron calculations cannot provide energies for the spectroscopic transitions, they are useful in visualizing the coefficient distributions in the frontier orbitals and providing a rough sequence of orbital energies. The geometry of the $\text{Cp}(\text{CO})\{\text{P}(\text{OMe})_3\}_3\text{M}\equiv\text{C}$ fragment was adapted from the X-ray structure of **1c**.² Due to conjugation of the phenyl ring with the metal-carbon π -system, rotation of the phenyl ring about the $\text{C}(\text{carbyne})-\text{C}(\text{ipso})$ bond affects the calculated energies. For these calculations, the plane of the phenyl ring is aligned with the $\text{W}-\text{P}$ bond so that the phenyl π -system is parallel to the $\text{W}-\text{CO}$ axis, as it is in the crystal structure of **1c**.

Figure 1 shows a partial molecular orbital diagram for the formation of **1a** from the fragments $\text{Cp}(\text{CO})\{\text{P}(\text{OMe})_3\}_3\text{W}^-$ and

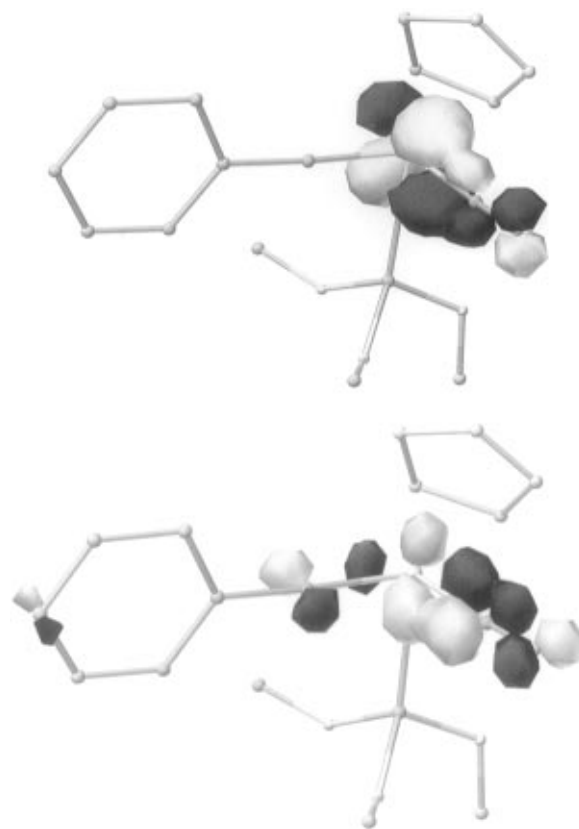


Figure 2. HOMO and LUMO of $\text{Cp}(\text{CO})\{\text{P}(\text{OMe})_3\}\text{W}\equiv\text{C}-\text{Ph}$ (**1a**). Coefficients are derived from extended Hückel calculations. Hydrogens and $-\text{OMe}$ groups are omitted for clarity. Key: (a, top) HOMO; (b, bottom) LUMO.

CPh^+ , calculated in the same manner as **1a**. The orbital orderings are similar to those previously reported for the model compound $\text{Cp}\{\text{P}(\text{OH})_3\}_2\text{Mo}\equiv\text{CPh}$,² although the energetic splittings are somewhat different. The HOMO of the complex (Figure 2) is comprised largely of the metal $d_{x^2-y^2}$ orbital but is partially devoted to back-bonding into the π^* orbital of the CO ligand. Below it are the two metal-carbon π bonds, their degeneracy broken by conjugation of the lower one with the phenyl ring. The LUMO is the orbital identified as the $\text{M}\equiv\text{C}$ π^* orbital that is conjugated into the phenyl π -system. However, inspection of Figure 2 reveals that it too is primarily composed of a metal d orbital delocalized into the π^* orbital of the CO ligand. The NLUMO is a nearly pure $\text{M}\equiv\text{C}$ π^* orbital. Extended Hückel calculations were also performed on the molybdenum compound **1b**, and the frontier orbitals obtained were very similar to those calculated for **1a**.

Assignment of the HOMO as a metal d orbital that is nonbonding with respect to the carbyne ligand is consistent with structural information obtained by X-ray crystallography on $\text{Br}(\text{dmpe})_2\text{W}\equiv\text{C}-\text{Ph}$ and its $1 e^-$ oxidized congener $[\text{Br}(\text{dmpe})_2\text{W}\equiv\text{C}-\text{Ph}][\text{PF}_6]$.¹⁰ Oxidation results in only a slight shortening of the $\text{W}-\text{C}(\text{carbyne})$ and $\text{W}-\text{Br}$ bonds (0.024 and 0.042 Å) while the $\text{W}-\text{P}$ bonds are lengthened somewhat. Upon this evidence, the HOMO is assigned as a nonbonding orbital that is primarily $d_{x^2-y^2}$ in character. Similar observations have been made for $\text{Cl}(\text{dppe})_2\text{Mo}\equiv\text{C}(p\text{-Tol})$ and $[\text{Cl}(\text{dppe})_2\text{Mo}\equiv\text{C}(p\text{-Tol})][\text{PF}_6]$.¹¹

This picture of the electronic structure of carbyne complexes **1a** and **1b** suggests that the lowest energy transition involves

(9) Extended Hückel calculations on **1a** were carried out using the CACHE WorkSystem Release 3.7, and iterative extended Hückel calculations on **1b** were run using the contained ZINDO package.

(10) Manna J.; Gilbert, T. M.; Dallinger, R. F.; Geib, S. J.; Hopkins, M. D. *J. Am. Chem. Soc.* **1992**, *114*, 5870–5872.

(11) Mortimer, M. D. Ph.D. Thesis, University of Bristol, 1991.

Table 1. Absorption Spectra of Cp(CO){P(OMe)₃}M≡C-R in THF Solution^a

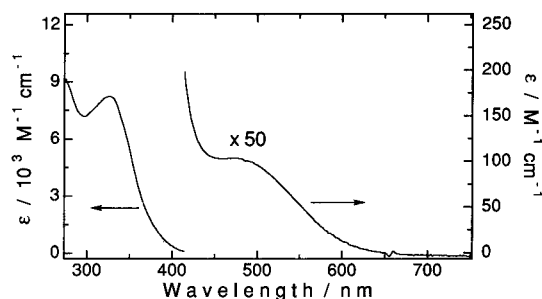
structure	M	R	λ_{\max}/nm (10^3 cm^{-1})	$\epsilon_{\max}/\text{M}^{-1} \text{ cm}^{-1}$	assignment	ref
1a	W	Ph	329 (30.4)	8000	$\pi(\text{W}\equiv\text{C}-\text{Ph}) \rightarrow \pi^*(\text{W}\equiv\text{C}-\text{Ph})$	2
			483 (20.7)	50	$d(\text{W}) \rightarrow \pi^*(\text{W}\equiv\text{C}-\text{Ph})$	
1b	Mo	Ph	328 (30.5)	4000	$\pi(\text{Mo}\equiv\text{C}-\text{Ar}) \rightarrow \pi^*(\text{Mo}\equiv\text{C}-\text{Ar})$	2
			477 (20.9)	60	$d(\text{Mo}) \rightarrow \pi^*(\text{Mo}\equiv\text{C}-\text{Ph})$	
1c	W	<i>o</i> -Tol	331 (30.2)		$\pi(\text{W}\equiv\text{C}-o\text{-Tol}) \rightarrow \pi^*(\text{W}\equiv\text{C}-o\text{-Tol})$	2
			476 (21.0)		$d(\text{W}) \rightarrow \pi^*(\text{W}\equiv\text{C}-o\text{-Tol})$	
1d	W	2-Np	348 (28.7)	6000	$\pi(\text{W}\equiv\text{C}-\text{Np}) \rightarrow \pi^*(\text{W}\equiv\text{C}-\text{Np})$	<i>b</i>
			490 (20.4)	70	$d(\text{W}) \rightarrow \pi^*(\text{W}\equiv\text{C}-\text{Ph})$	

^a λ_{\max} and τ_{em} values for **1a–c** are reported in ref 2. ^b This work.

Table 2. Luminescence and Transient Absorption Data for Cp(CO){P(OMe)₃}M≡C-R^{a,b}

structure	M	R	298 K ^c						77 K ^d	
			λ_{\max}/nm (10^3 cm^{-1})	$\tau_{\text{em}}/\text{ns}$ ^e	Φ_{em}	k_r/s^{-1}	$k_{\text{nr}}/\text{s}^{-1}$	$\tau_{\text{TA}}/\text{ns}$	λ_{\max}/nm (10^3 cm^{-1})	$\tau_{\text{em}}/\mu\text{s}$
1a	W	Ph	747 (13.4)	141	6.9×10^{-4}	4.9×10^3	7.8×10^6	129	741 (13.5)	3.2
1b	Mo	Ph	<i>f</i>	<i>f</i>	$< 10^{-4}$	$< 2 \times 10^3$	2.0×10^7 ^g	49	787 (12.7)	8.3
1c	W	<i>o</i> -Tol	745 (13.4)	170	3.6×10^{-4}	2.1×10^3	5.9×10^6		735 (13.6)	3.6
1d	W	2-Np	> 780 (< 12.7)	66			1.5×10^7	60		

^a λ_{\max} = emission maximum; τ_{em} = emission lifetime; Φ_{em} = emission quantum yield; k_r = radiative decay rate; k_{nr} = nonradiative decay rate; τ_{TA} = transient absorption decay lifetime. ^b Estimated errors: τ_{em} , $\pm 5\%$; Φ_{em} , $\pm 15\%$; k_r , $\pm 20\%$; k_{nr} , $\pm 5\%$; τ_{TA} , $\pm 5\%$. ^c Argon-degassed THF solutions. ^d Argon-degassed 2-MeTHF glasses. ^e λ_{\max} and τ_{em} values for **1a–c** are reported in ref 2. See text. ^f Too weak for accurate determination. ^g Determined from the decay rate of excited state absorption.

**Figure 3.** Absorption spectrum of Cp(CO){P(OMe)₃}W≡C-Ph in THF solution at room temperature.

the frontier orbitals depicted in Figure 2. This is the transition identified in prior literature as $d(\text{M}) \rightarrow \pi^*(\text{M}\equiv\text{C}-\text{Ar})$ MLCT in nature.^{1–3} Although this transition does involve some charge transfer to the carbyne ligand, the earlier designation of “MLCT” suggests a higher degree of charge transfer and higher band intensity than is actually observed (*vide infra*). Both the HOMO and the LUMO are primarily composed of the metal d orbitals and the carbonyl π^* orbitals. As a result, the lowest energy transition has a considerable degree of d–d character that is consistent with its low extinction coefficient.

Electronic Absorption Spectra. Figure 3 illustrates the absorption spectrum of tungsten carbyne **1a** in THF solution, which is typical for the series of metal carbynes examined herein, and Table 1 summarizes the data and assignments for the entire set of complexes. The absorption spectra of the aryl-substituted carbynes **1a–c** exhibit two primary UV/visible absorption features: a strong band at approximately 330 nm and a weaker broad absorption at about 480 nm. The absorption spectrum of naphthylcarbyne **1d** showed slight red shifts of both bands, but otherwise was similar.

The low-energy absorptions are clearly related to those assigned as $d \rightarrow \pi^*$ MLCT for the similar compounds $\text{X}(\text{CO})_2\text{L}_2\text{W}\equiv\text{C}-\text{R}$ (R = Ph, ^tBu; X = Cl, Br; L₂ = TMEDA, 2py, dppe).¹ As discussed above, these transitions in **1a–d** contain substantially more d → d character than the description “MLCT” implies, but to maintain continuity with earlier literature we will use that assignment periodically while emphasizing that the actual excited states are not pure MLCT. The d–d character of the low-energy absorption in **1a–c** (and

by inference in **1d**) is underscored by previous studies from our laboratory which demonstrated that the absorption band is not solvatochromic.² The more intense absorption at 330 nm is assigned to $\pi \rightarrow \pi^*$ transitions of the $\text{M}\equiv\text{C}-\text{Ar}$ chromophore. While there is a significant energy gap between the visible and near-UV transitions, the extended Hückel calculations are in qualitative agreement with these assignments. The slight red shifts for the naphthylcarbyne can be attributed to mixing of the larger π system with the LUMO, lowering its energy.

Luminescence Studies. Detailed steady state and time resolved luminescence studies were carried out on complexes **1a–d**. The fluorescence detection system was corrected for monochromator and photomultiplier response to 800 nm, but owing to the sharp decrease in the efficiency of the detector at wavelengths greater than 800 nm, we were unable to collect useful luminescence data beyond this wavelength. This point is significant, because the emission of the W and Mo carbyne complexes extends well into the near-IR (*vide infra*).

Each of the tungsten carbyne complexes luminesces weakly in solution at 298 K. Table 2 provides a summary of the emission parameters, including wavelength maxima (λ_{\max}) for the corrected emission bands, and emission quantum efficiencies and lifetimes (Φ_{em} and τ_{em} , respectively). Where possible, radiative and nonradiative decay rate constants (k_r and k_{nr} , respectively) were calculated by the expressions $k_r = \Phi_{\text{em}}/\tau_{\text{em}}$ and $k_{\text{nr}} = (1/\tau_{\text{em}} - k_r)$. Note that by applying these expressions we assume that the luminescent state is reached with unit quantum efficiency.

In fluid solution at 298 K the most pronounced emission is observed from tungsten complexes **1a** and **1c**. Emission from these complexes is very similar, appearing as a broad, structureless band in the red with $\lambda_{\max} \approx 745$ nm (Figure 4a).¹² In each case the luminescence efficiency is rather low, with $\Phi_{\text{em}} \approx 5 \times 10^{-4}$ (Table 2). Emission excitation spectra for **1a** and **1c** are also illustrated in Figure 4a and reveal that the red luminescence is produced by excitation of the visible and near-UV absorption bands. Emission lifetimes for **1a** and **1c** are comparable, and indicate that the luminescent excited state has a lifetime in the 100–200 ns range at room temperature.

(12) These emission maxima are longer than previously reported² because the earlier spectra were obtained without correcting for monochromator/detector response.

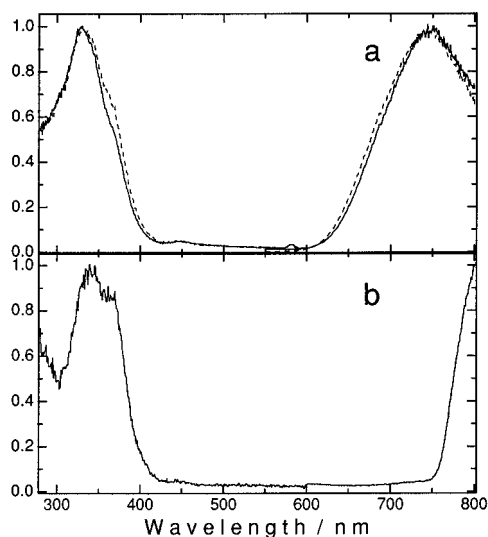


Figure 4. Emission and emission excitation spectra for tungsten carbyne complexes in THF solution at room temperature. Emission spectra are at right and excitation spectra at left. Key: (a) $\text{Cp}(\text{CO})\{\text{P}(\text{OMe})_3\}\text{W}\equiv\text{C}-\text{Ph}$ (solid line) and $\text{Cp}(\text{CO})\{\text{P}(\text{OMe})_3\}\text{W}\equiv\text{C}-o\text{-tol}$ (dashed line); (b) $\text{Cp}(\text{CO})\{\text{P}(\text{OMe})_3\}\text{W}\equiv\text{C}-2\text{-Np}$.

The emission of **1a** and **1c** was also examined at 77 K in a 2-MTHF solvent glass, and the maxima and lifetimes for the low temperature luminescence are listed in Table 2. The emission of both complexes at low temperature appears as a broad band which is similar in energy and bandshape to that observed in fluid solution at 298 K. Thus, luminescence “rigidochromism”, which is typically observed for charge transfer excited states, was not apparent for **1a** and **1c**. This effect underscores the small degree of MLCT character in the luminescent excited state for the carbyne complexes. The 77 K emission lifetimes for the two tungsten complexes are similar, and are comparable to the lifetimes observed at 77 K for d–d excited states in $\text{W}(\text{CO})_5\text{L}$ complexes.¹³

At 298 K in fluid solution the 2-naphthylcarbyne complex **1d** exhibits an emission which is substantially red-shifted relative to that of the phenyl and *o*-tolyl complexes. Owing to the large red shift, our instrument is only capable of detecting the blue edge of the band (Figure 4b), and λ_{max} for **1d** is apparently >800 nm. An emission excitation spectrum of **1d** obtained with $\lambda_{\text{em}} = 790$ nm is also illustrated in Figure 4b. There is good agreement between the absorption and excitation spectra for **1d**, which confirms that the near-IR emission indeed emanates from the complex. The lifetime of the near-IR emission of **1d** was determined to be 66 ns, which is slightly shorter than the lifetimes for the phenyl and *o*-tolyl complexes.

Molybdenum carbyne **1b** exhibits no detectable luminescence at 298 K. However, at 77 K in 2-MTHF the complex features a broad, structureless emission band that is similar in bandshape but red-shifted compared to the emission of the tungsten analog **1a** (Table 2). The emission band decreases in intensity as the temperature of the MTHF solution is increased above the glass-to-fluid transition (100–120 K) at which point the luminescence becomes too weak to detect ($\Phi_{\text{em}} < 10^{-4}$). The emission lifetime of **1b** at 77 K (8.3 μs) is slightly longer than that of the tungsten analog.

Transient Absorption Spectroscopy. Nanosecond laser flash photolysis studies were carried out on carbyne complexes **1a**, **1b**, and **1d** in argon-degassed THF solutions. All experi-

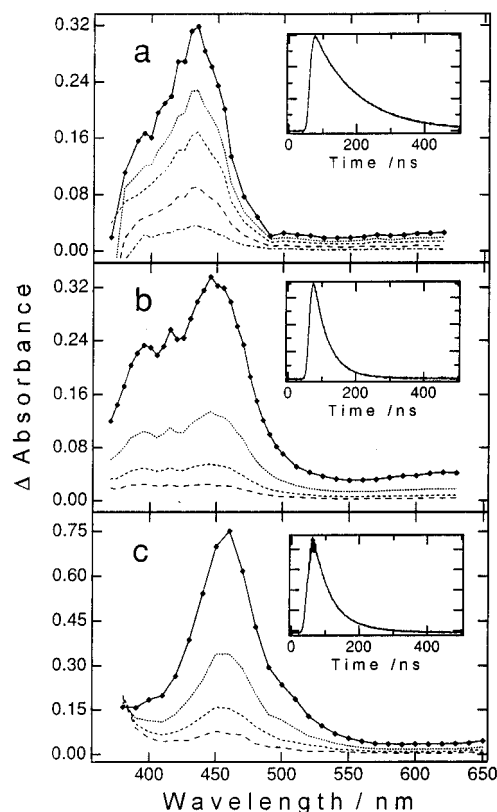


Figure 5. Transient absorption difference spectra following laser excitation (355 nm, 10 ns fwhm, 10 mJ/pulse). Key: (a) $\text{Cp}(\text{CO})\{\text{P}(\text{OMe})_3\}\text{W}\equiv\text{C}-\text{Ph}$ in THF solution, where delay times range from 0 to 280 ns (inset: Transient absorption kinetics at 430 nm); (b) $\text{Cp}(\text{CO})\{\text{P}(\text{OMe})_3\}\text{Mo}\equiv\text{C}-\text{Ph}$ in THF solution, where delay times range from 0 to 120 ns (inset: Transient absorption kinetics at 445 nm); (c) $\text{Cp}(\text{CO})\{\text{P}(\text{OMe})_3\}\text{W}\equiv\text{C}-2\text{-Np}$ in THF solution, where delay times range from 0 to 160 ns (inset: Transient absorption kinetics at 460 nm).

ments were performed by using the third harmonic output of a Nd:YAG laser for excitation (355 nm, 10 ns fwhm, 10 mJ/pulse). As described below, strongly absorbing transients were observed for each complex, and the decay lifetimes for the transient absorptions were determined by global kinetic analysis of the transient absorption decay at >25 wavelengths.¹⁴

Figure 5a illustrates transient absorption difference spectra of **1a** at delay times ranging from 0 to 280 ns following laser excitation. The spectra are characterized by a broad absorption band with $\lambda_{\text{max}} \approx 440$ nm. There appears to be a hint of structure on the absorption band, with distinct (and reproducible) shoulders at 395, 420, and 460 nm. Global analysis of the transient absorption data indicates that the transient decays with a lifetime of 129 ns, in good agreement with the previously reported emission lifetime ($\tau_{\text{em}} = 141$ ns).¹⁵ The correspondence of the transient absorption and emission lifetimes strongly implies that the transient absorption is due to the luminescent excited state. Under the assumption that the lowest excited state

(13) (a) Lees, A. J. *J. Am. Chem. Soc.* **1982**, *104*, 2038. (b) Lees, A. J.; Adamson, A. W. *J. Am. Chem. Soc.* **1982**, *104*, 3804. (c) Lees, A. J. *Chem. Rev.* **1987**, *87*, 711.

(14) (a) SPECFIT (v 1.17), Spectrum Software Associates, Chapel Hill, NC, 1994. (b) Stultz, L. K.; Binstead, R. A.; Reynolds, M. S.; Meyer, T. J. *J. Am. Chem. Soc.* **1995**, *114*, 2520–2532.

(15) The emission lifetime of **1a** which is listed in Table 2 and was previously reported in ref 2 was determined by using a pulsed laser technique. We have measured the emission lifetime of **1a** in THF by using time-correlated single photon counting (TCSPC), which is a more precise and accurate method for obtaining emission lifetimes for weakly emissive samples as compared to the pulsed laser technique used in the previous study. The emission lifetime of **1a** determined by TCSPC is 129 ns, in excellent agreement with the transient absorption decay lifetime.

of **1a** is populated with unit efficiency following 355 nm excitation, it is possible to determine the difference molar absorptivity ($\Delta\epsilon$) of this state by using the relative actinometry method.¹⁶ This experiment was accomplished by using [*fac*-(2,2'-bipyridine)Re(CO)₃(4-benzylpyridine)]⁺ as an actinometer ($\Delta\epsilon = 11\,200\text{ M}^{-1}\text{ cm}^{-1}$ at 370 nm)¹⁷ and led to a value of $\Delta\epsilon = 3000\text{ M}^{-1}\text{ cm}^{-1}$ at 440 nm for **1a**.

Figure 5b illustrates transient absorption difference spectra of **1b** at delay times ranging from 0 to 120 ns following laser excitation. The spectrum of this complex is characterized by a moderately intense and broad absorption band with $\lambda_{\text{max}} \approx 445$ nm, with distinct (and reproducible) shoulders at 395 and 420 nm. Global analysis of the transient absorption data indicates that the transient decays with a lifetime of 49 ns. The close correspondence between the transient absorption spectra of **1a** and **1b** points to a similar electronic structure for the absorbing excited states in both complexes.

Figure 5c illustrates the transient absorption difference spectra of naphthylcarbyne complex **1d** at delay times ranging from 0 to 160 ns delay following excitation. The spectra are characterized by an intense but featureless transient absorption band with $\lambda_{\text{max}} \approx 460$ nm. Global analysis of the transient absorption data indicates that the transient decays with a lifetime of 60 ns in very good agreement with the emission lifetime of the complex (66 ns). The agreement between the transient absorption and emission decay lifetimes suggests that for **1d** the transient absorption arises from the luminescent excited state.

Discussion

Photophysics of Metal Carbyne Complexes. During the past decade there have been a number of photophysical studies of complexes that contain the metal-arylcarbyne functionality, $\text{M}\equiv\text{C}-\text{Ar}$, where $\text{M} = \text{W}(\text{IV}), \text{Mo}(\text{IV}),$ and $\text{Os}(\text{IV})$.^{1-3,10,18} This family of complexes displays remarkably similar absorption and luminescence properties, despite having a rather wide variety of ancillary ligands in the coordination environment.^{1-3,10} In general, the absorption of $\text{M}\equiv\text{C}-\text{Ar}$ complexes is characterized by a weak band in the 400–500 nm region ($\epsilon \approx 10^2\text{ M}^{-1}\text{ cm}^{-1}$) and a more intense band between 300 and 350 nm ($\epsilon \approx 10^4\text{ M}^{-1}\text{ cm}^{-1}$). Theoretical and spectroscopic studies indicate that the low energy band is associated with the HOMO \rightarrow LUMO transition, which is dominated by the $\text{d}(\text{M}) \rightarrow \pi^*(\text{M}\equiv\text{C}-\text{Ar})$ configuration.^{1-3,10,19} The low intensity of the HOMO \rightarrow LUMO transition indicates that it is forbidden; the transition is likely parity forbidden but spin-allowed (i.e., a singlet-singlet transition). The transition is parity forbidden owing to significant degree of d-character in the HOMO and LUMO. The more intense near-UV band is associated with a spin-allowed $\pi(\text{M}\equiv\text{C}-\text{Ar}) \rightarrow \pi^*(\text{M}\equiv\text{C}-\text{Ar})$ transition, which bears some analogy to the $\pi \rightarrow \pi^*$ transition of the $\text{Ph}-\text{C}\equiv\text{C}-\text{Ph}$ chromophore.

There are also several reports of luminescence from complexes that contain the $\text{M}\equiv\text{C}-\text{Ar}$ functionality.¹⁻³ For example, complexes of the type $\text{X}(\text{CO})_2(\text{L})_2\text{W}\equiv\text{C}-\text{Ph}$ and $[\text{Ph}-\text{C}\equiv\text{Os}(\text{NH}_3)_5]^{3+}$ exhibit weak luminescence in the 600–650 nm region which has been attributed to the $\text{d}(\text{M}) \rightarrow \pi^*(\text{M}\equiv\text{C}-\text{Ar})$ excited

state. The emission lifetime of these complexes ranges from 50 to 250 ns, with quantum yields typically on the order of 5×10^{-4} . The comparatively long excited state lifetimes coupled with relatively low radiative rates ($k_r \approx 10^3\text{ s}^{-1}$) strongly imply that the luminescent state has triplet spin character. This assertion has been confirmed in several cases by the observation of triplet energy transfer from a carbyne excited state to organic triplet state acceptors.^{1b,3} The triplet character of the luminescent state in the carbyne complexes explains the large Stokes shift of the emission relative to the low intensity absorption in the mid-visible region, which is assigned to the spin-allowed (singlet-singlet) absorption.

Photophysics of $\text{W}\equiv\text{C}-\text{Ar}$ and $\text{Mo}\equiv\text{C}-\text{Ph}$ Complexes. Complexes **1a-d** display absorption features (see Table 1) that bear a strong similarity to those described above for the structurally related arylcarbyne complexes. These features include a weak absorption with λ_{max} located between 475 and 500 nm which is assigned to the parity-forbidden, spin-allowed (i.e., singlet-singlet) $\text{d}(\text{M}) \rightarrow \pi^*(\text{M}\equiv\text{C}-\text{Ar})$ transition as well as a moderately intense absorption in the near-UV between 325 and 350 nm which is assigned to the spin-allowed $\pi(\text{M}\equiv\text{C}-\text{Ar}) \rightarrow \pi^*(\text{M}\equiv\text{C}-\text{Ar})$ transition.

The luminescence features of the tungsten and molybdenum carbynes studied herein also are similar to those of related arylcarbyne complexes. Thus, tungsten carbynes **1a**, **1c**, and **1d** all display weak luminescence in the red, with emission lifetimes in fluid solution ranging from 60 to 170 ns. The molybdenum phenylcarbyne complex **1b** is not luminescent at room temperature in fluid solution; however, red luminescence is observed when the compound is frozen in a glassy matrix at 77 K. By analogy to the previously reported arylcarbyne complexes, the luminescence observed from **1a-d** is attributed to the $\text{d}(\text{M}) \rightarrow \pi^*(\text{M}\equiv\text{C}-\text{Ar})$ triplet state. The triplet assignment has been substantiated in **1a** by previously reported triplet energy transfer studies.² The significant Stokes shift of the emission from **1a**, **1c**, and **1d** relative to the low-intensity visible absorption band ($\approx 7.0 \times 10^3\text{ cm}^{-1}$) is attributed to the fact that the absorption is due to the singlet-singlet HOMO-LUMO transition, while the emission emanates from the triplet spin manifold arising from the HOMO-LUMO transition. The Stokes shift observed for these carbyne complexes is similar to that reported for ³d-d luminescence in tungsten and molybdenum carbonyl complexes of the type $\text{M}(\text{CO})_5\text{L}$.¹³ Of further interest is the fact that the luminescence data presented herein argues against the suggestion made earlier that the large Stokes shift may be partly due to geometry changes associated with excitation of the $\text{M}\equiv\text{C}-\text{Ar}$ functionality.^{1b} The lack of a significant difference in the emission energy or bandshape for **1a** and **1c** in fluid solution compared to in rigid glass at 77 K implies that there is no substantial inner- or outer-sphere reorganization associated with the optical excitation.

Despite the overall similarities of the absorption and luminescence properties of **1a-d**, there are important distinctions that provide insight concerning the nature of the electronic states involved in the photophysics. First, the visible and near-UV absorption bands and the luminescence of the 2-Np complex **1d** are noticeably red-shifted compared to those for the phenyl and *o*-tolyl analogs. The red-shift of both absorption bands and the luminescence in the 2-Np complex is expected, since the naphthalene ring provides extended conjugation for the $\pi^*(\text{M}\equiv\text{C}-\text{Ar})$ orbital, which is the LUMO of the complex and is the "acceptor" orbital for the visible and near-UV π, π^* transitions.

Second, the tungsten and molybdenum phenylcarbyne analogs **1a** and **1b** display remarkably similar ground- and excited-state

(16) Carmichael, I.; Hug, G. L. *J. Phys. Chem. Ref. Data* **1986**, *15*, 1–250.

(17) Lucia, L. A.; Schanze, K. S. *Inorg. Chim. Acta* **1994**, *225*, 41–49.

(18) These assignments of formal oxidation state follow the convention of counting the carbyne ligand as CR^{3-} , without regard for the reactivity of the complex. The spectral data and reactivity of **1a-d** more closely resemble the low-valent Fischer carbynes than higher valent alkylidyne complexes.

(19) (a) Kostic, N. M.; Fenske, R. F. *J. Am. Chem. Soc.* **1981**, *103*, 4677–4685. (b) Kostic, N. M.; Fenske, R. F. *Organometallics* **1982**, *1*, 489–496.

absorption spectra. This likeness points to a similarity in the electronic structure of the two complexes. The one notable difference in the photophysical properties of the two phenylcarbynes is the lack of observable luminescence from **1b** in fluid solution at room temperature. Since the excited state lifetimes of **1a** and **1b** are not significantly different (i.e., from transient absorption 130 and 50 ns for **1a** and **1b**, respectively), the lower emission yield of **1b** in fluid solution indicates a lower radiative decay rate. The lower radiative decay rate of **1b** might be attributed to lower spin-orbit coupling (and therefore less singlet-triplet mixing) in the Mo complex as compared to the W analog.

A distinguishing feature of the present study is the observation of strong transient absorption by the $d(M) \rightarrow \pi^*(M\equiv C-Ar)$ excited states of the tungsten and molybdenum arylcarbynes. To our knowledge, this is the first report of transient absorption spectra of photoexcited Fischer carbyne complexes. There are several important ramifications of the observation of transient absorption signals for the excited states of this family of complexes. First, as noted above, it is clear that the excited state carbynes have comparatively large difference molar absorptivities. This is in contrast with the low molar absorptivity that is typical of $d-d$ excited states of organometallic complexes.^{20,21} The moderate to large difference molar absorptivity of the excited states of the arylcarbyne complexes is more in accord with that of $d\pi(M) \rightarrow \pi^*(\text{ligand})$ MLCT excited states in d^6 metal diimine complexes such as $Ru(\text{bpy})_3^{2+}$ and $[(\text{bpy})\text{-Re}^I(\text{CO})_3(\text{py})]^{1+}$ ($\text{bpy} = 2,2'$ -bipyridine and $\text{py} = \text{pyridine}$).^{17,22}

An important question concerns the origin of the moderate to strong absorbance of the $d \rightarrow \pi^*$ excited states in the arylcarbyne complexes. The absorption of MLCT excited states in d^6 metal diimine complexes has been assigned to spin-allowed $\pi^* \rightarrow \pi^*$ and $\pi \rightarrow \pi$ transitions of the diimine radical anion chromophore that is produced by MLCT excitation.²³ By analogy, the absorption of the $d \rightarrow \pi^*$ excited state in the arylcarbyne complexes may be associated with an allowed $\pi^* \rightarrow \pi^*$ transition of the $M\equiv C-Ar$ chromophore. In this connection, it is important to note that the excited state absorption of phenylcarbyne complexes **1a** and **1b** is quite similar, while that of naphthylcarbyne **1b** is slightly red shifted (and qualitatively appears to be more intense). The red shift in the naphthyl system suggests the involvement of the π or π^* levels of the aryl unit in the optical transition detected in the transient absorption experiment.

Finally, the substantial difference absorptivity of the excited state in the arylcarbyne complexes provides an exceedingly useful means to track the excited state dynamics (and reactivity). This is significant, because even though emission studies have provided an opportunity to study the excited states of certain metal carbynes, the method has limitations. For example, among **1a-d** and related $\text{Cp}(\text{CO})_2\text{M}\equiv\text{C}-\text{R}$ and $\text{Cp}\{\text{P}(\text{OMe})_3\}_2\text{M}\equiv\text{C}-\text{R}$ species, only the tungsten arylcarbynes with one phosphite ligand and one CO ligand display easily observable luminescence. Even for these complexes, the luminescence efficiency is low, as evidenced by the quantum yield for emission for **1a** and **1c**. The bis(phosphite) arylcarbynes are not emissive in solution at room temperature,² while molybdenum complex **1b** is nonluminescent under the same experimental conditions. Comparing the lifetime measurements

obtained by absorbance with those observed by the emission method provides assurance that the observed transients are in fact the emissive states. Furthermore, by applying global analysis to the transient absorption data, it is in principle possible to obtain very reliable excited state decay rate data.¹⁴

Conclusion

Low-valent carbyne complexes are well established compounds in organometallic chemistry, yet relatively few photophysical studies on these complexes have appeared in the literature. In this work, the complexes $\text{Cp}(\text{CO})\{\text{P}(\text{OMe})_3\}\text{M}\equiv\text{C}-\text{R}$ ($\text{M} = \text{Mo}, \text{W}$; $\text{R} = \text{Ph}, o\text{-Tol}, 2\text{-Np}$) (**1a-d**) were examined in an effort to learn more about the excited states of these molecules, as well as to provide some information relevant to the study of photochemical reactions. Extended Hückel calculations and absorbance spectra indicate that **1a-d** possess low-lying excited states which can be populated directly via a parity-forbidden, singlet-singlet optical transition in the mid-visible region. Emission is observed from the triplet manifold of these excited states, and at room temperature in fluid solution the lifetimes of the triplet states range from 50 ns for the molybdenum phenylcarbyne **1b** to 170 ns for the tungsten tolylcarbyne **1c**. Transient absorbance measurements performed on **1a-d** in THF indicate that the triplet excited states can also be detected and monitored by absorption, since the lifetimes obtained in the absorbance experiments match those obtained through emission methods. The observation of strong excited state absorption provides an avenue for future work concerning the photophysics and photochemistry of arylcarbyne complexes. Such work may include studies of excited state electron transfer quenching by acceptors and excited state resonance Raman to provide further information concerning the nature of the excited states.

Experimental Section

General Methods. Standard inert atmosphere techniques were used throughout. Et_2O , THF, and toluene were distilled from $\text{Na}/\text{Ph}_2\text{CO}$. Hexane, CHCl_3 (ethanol free unless stated), and methylene chloride were distilled from CaH_2 . CDCl_3 was degassed by three freeze-pump-thaw cycles and stored over 3 Å molecular sieves. All other starting materials were purchased in reagent grade and used without further purification. The carbyne complexes **1a-c** were synthesized by methods described previously.^{2,8}

Equipment and Instrumental Methods. ^1H , ^{13}C , and ^{31}P NMR spectra were recorded on Varian XL-300 and VXR-300 NMR spectrometers. ^1H NMR spectra are referenced to the residual protons of the deuterated solvent. ^{31}P NMR spectra are referenced to 85% $\text{H}_3\text{-PO}_4$ and are proton decoupled. IR spectra were recorded on a Perkin-Elmer 1600 spectrometer. A Hewlett-Packard 8452A diode array spectrophotometer was used to obtain UV-visible absorption spectra. Corrected emission and emission excitation spectra were obtained with a Spex Industries F-112A spectrophotometer. Emission correction factors were generated by using a 1000 W tungsten primary standard lamp. Emission quantum yields are reported relative to aqueous $\text{Ru}(\text{bpy})_3^{2+}$ ($\Phi_{\text{em}} = 0.055$).²⁴ All room temperature measurements were carried out on argon-degassed THF solutions and studies at low temperature were conducted on argon-degassed 2-methyltetrahydrofuran (MTHF) solutions.

The instrumentation for the emission lifetime measurement on **1c** has been described previously.²⁵ Other emission lifetimes were measured on a Photochemical Research Associates time-correlated single photon counting spectrophotometer, which relies on an H_2 gas-filled spark gap for an excitation source. For emission decay experi-

(20) Creutz, C.; Chou, M.; Netzel, T. L.; Okumura, M.; Sutin, N. *J. Am. Chem. Soc.* **1980**, *102*, 1309-1319.

(21) Langford, C. H.; Malkhasian, A. Y. S.; Sharma, D. K. *J. Am. Chem. Soc.* **1984**, *106*, 2727-2728.

(22) Ohno, T.; Yoshimura, A.; Prasad, D. R.; Hoffman, M. Z. *J. Phys. Chem.* **1990**, *94*, 4871-4876.

(23) Watts, R. J. *J. Chem. Educ.* **1983**, *60*, 834-842.

(24) Harriman, A. *J. Chem. Soc., Chem. Commun.* **1977**, 777-778.

(25) (a) Tro, N. J.; Haynes, D. R.; Nishimura, A. M.; George, S. M. *J. Chem. Phys.* **1989**, *91*, 5778-5785. (b) Haynes, D. R.; Helwig, K. R.; Tro, N. J.; George, S. M. *J. Chem. Phys.* **1990**, *93*, 2836-2847.

ments excitation light was filtered using a colored glass filter (Schott, UG-11) and emission light was filtered using interference filters at 650, 700, or 750 nm. Emission decay analysis was carried out using the DECAN deconvolution software.²⁶ Laser flash photolysis experiments were carried out on a system that has been described previously.²⁷ Global analysis of the multiwavelength transient absorption data was effected using the SPECFIT factor analysis software.¹⁴

[(CO)₅WC(O)(2-naphthyl)][NMe₄] (3d). 2-Naphthyl bromide (4.0 g, 19 mmol) was dissolved in 60 mL of THF and cooled to -78 °C. *n*-Butyllithium (2.0 M in pentane, 10 mL) was added under nitrogen, and a yellow suspension was observed. After the solution was allowed to stir for 1 h, the entire solution was transferred by cannula to a flask containing W(CO)₆ (6.75 g, 19 mmol) in THF at -78 °C. The resulting red solution was allowed to stir for 2.5 h at -78 °C, and then the THF was removed under vacuum, leaving a red oily-solid which was recrystallized from Et₂O/hexanes to yield a red crystalline solid. The solid was dissolved in 30 mL of degassed H₂O, and the mixture was filtered through a fritted funnel into a solution containing NMe₄Br (7.4 g, 48 mmol). The solution separated into two layers, and the top layer was removed via cannula. The remaining red oil was placed under vacuum to remove any additional H₂O and used without further purification (9.3 g, 88%). ¹H NMR (CDCl₃): δ 7.4–8.0 (m, 7H), 2.25 (s, 12H).

Cl(CO){P(OMe)₃}₃W≡C(2-naphthyl) (2d). Acyl complex **3d** (9.3 g, 17 mmol) was dissolved in 70 mL of CH₂Cl₂ and cooled to -95 °C. Oxalyl chloride (2.2 g, 17 mmol) was added, the solution was allowed to warm to -20 °C, and evolution of gas was observed. After the solution was cooled once more to -95 °C, trimethyl phosphite was

added (16.7 g, 135 mmol), and when it warmed to room temperature, more effervescence occurred. The mixture was then refluxed for 24 h, after which the solvent and excess P(OMe)₃ were removed under vacuum. The remaining red oily solid was dissolved in Et₂O and passed through a fritted funnel containing neutral alumina. The Et₂O was removed under vacuum, leaving **2d** as a red oil in 58% yield. ¹H NMR (CDCl₃): δ 7.4–7.9 (m, 7H), 3.6 (m, 27H).

Cp(CO){P(OMe)₃}₃W≡C(2-naphthyl) (1d). Tris(phosphite) complex **2d** (2.9 g, 3.8 mmol) was dissolved in 45 mL of THF, and CpNa (2.0 M in THF, 4.0 mL) was added. The dark red solution was refluxed for 24 h, after which THF and P(OMe)₃ were removed under vacuum. The resulting dark oil was dissolved in Et₂O and passed through a short alumina column to remove unreacted CpNa. After the solvent was removed, the red oil was placed on a longer alumina column and washed with hexane. The yellow eluent was discarded, and further elution with 1:2 Et₂O/hexane gave a red solution which was concentrated to give **1d** as a red oil in 20% yield. ¹H NMR (CDCl₃): δ 7.81 (s, 1H), 7.76 (d, 1H), 7.69 (d, 1H), 7.59 (d, 1H), 7.42 (m, 3H), 5.57 (s, 5H, Cp), 3.61 (d, *J*_{HP} = 12.0 Hz, 9H, [P(OMe)₃]). ¹³C NMR (CDCl₃): δ 286.5 (d, *J*_{CP} = 18.2 Hz, W≡C), 235.3 (d, *J*_{CP} = 9.7 Hz, CO), 150.0 (s, ≡C–C), 133.0, 131.9 (bridge), 127.8, 127.7, 127.2, 126.9, 126.8, 126.4, 125.8 (Np), 90.0 (s, Cp), 52.4 (d, *J*_{CP} = 2.4 Hz, P{OMe}₃). ³¹P NMR (CDCl₃): δ 173.0 (*J*_{WP} = 662 Hz). IR (CH₂Cl₂): 1888 cm⁻¹ (*ν*_{WCO}). UV (THF): 348 (ε = 6000), 490 (ε = 70) nm. HRMS (FAB), *m/z*: calcd for M⁺ (C₂₀H₂₁O₄PW), 540.0687; found, 540.0619.

Acknowledgment. L.M.W. and K.S.S. acknowledge financial support for this work from the National Science Foundation (L.M.W.: Grants CHE-9396213 and CHE-9421434; K.S.S.: Grant CHE-9401620).

(26) De Roeck, R.; Boens, N.; Dockx, J. DECAN (version 1.0), K. U. Leuven, Belgium, 1990.

(27) Wang, Y.; Schanze, K. S. *Chem. Phys.* **1993**, *176*, 305–319.